Thermoelectric power and electrical resistivity of crystalline antimony telluride (Sb2Te3) thin films: Temperature and size effects

V. Damodara Das and N. Soundararajan

Citation: J. Appl. Phys. 65, 2332 (1989); doi: 10.1063/1.342823
View online: http://dx.doi.org/10.1063/1.342823
View Table of Contents: http://jap.aip.org/resource/1/JAPIAU/v65/i6
Published by the AIP Publishing LLC.

Thermoelectric power and electrical resistivity of crystalline antimony telluride (Sb_2Te_3) thin films: Temperature and size effects

V. Damodara Das and N. Soundararajan
Thin Film Laboratory, Department of Physics, Indian Institute of Technology, Madras 600 036, India

(Received 18 September 1987; accepted for publication 9 November 1988)

Crystalline Sb_2Te_3 thin films of different thicknesses have been prepared by subsequent annealing (at 500 K) of vacuum deposited, as-grown, amorphous thin films of Sb_2Te_3 prepared on glass substrates at room temperature. Thermoelectric power and electrical resistivity of these annealed (crystalline) films have been determined as a function of temperature. The size dependence of thermoelectric power and electrical resistivity have been analyzed by the effective mean free path model of size effect. It is found that both the thermoelectric power and the electrical resistivity are linear functions of the reciprocal of thickness of the films. The data from the analyses of thermoelectric power and electrical resistivity have been combined to evaluate important material parameters such as carrier concentration, their mean free path, Fermi energy, and effective mass. The values of some of these are compared with the previous available values from literature.

I. INTRODUCTION

Antimony telluride is a narrow band-gap semiconductor and has been the subject of great interest during recent years owing to its potential application as a thermoelectric material. Antimony telluride is rhombohedral and belongs to the space group $R\,\bar{3}m$. The structure is comprised of alternate layers of antimony and tellurium atoms normal to the threefold axis. This results in anisotropy in many properties. It has been observed that the conductivity of antimony telluride is not susceptible to change in doping or to appreciable alterations in the proportion of antimony and tellurium. It becomes intrinsic at about 900 K. Solid solutions of antimony telluride with bismuth telluride give *p*-type materials with a higher thermoelectric figure of merit than either of the constituents alone. This is due to the reduction in the mean free path of phonons without similar reduction in the mean free path of holes.

Even though there is a fair amount of work done on Sb_2Te_3 regarding its electrical properties[1–11] in the bulk solid state and particularly on the thermoelectric behavior,[7–11] only very little work[12–14] has been reported on Sb_2Te_3 thin films, even though it is a good thermoelectric material.

For example, Rajagopalan and Ghosh[12] measured the Hall constant, the resistivity, and the Seebeck coefficient of thin films of thicknesses from 1600 to 8000 Å. They found that all the above parameters were thickness dependent. From their studies, it was found that thin films were *p* type.

Gadgil and Goswami[13] studied the epitaxial growth of thin films on single-crystal substrates like mica and rock salt, and Kremnev, Leont'ev, and Platov[14] investigated the structure changes as a function of substrate temperature.

The present studies were carried out in an attempt to make a detailed analysis of the behavior of Sb_2Te_3 thin films regarding the electrical conduction and thermoelectric properties. The size effects on Seebeck coefficient and resistivity of the films were analyzed using the effective mean-free-path model. Spline functions that are localized polynomials were used for the least-squares fitting of the data, instead of the usual nonlocalized function valid for the entire range. This avoids forcing the data to a preassigned relationship function. The analysis using the effective mean-free-path model results in the determination of the mean free path and its energy dependence. The analysis further leads to the determination of the parameters such as carrier concentration, effective mass, and Fermi energy.

II. EXPERIMENT

Sb_2Te_3 thin films of different thicknesses (500–2000 Å) were prepared by the vacuum evaporation of the bulk alloy Sb_2Te_3. A bulk Sb_2Te_3 alloy for evaporation was prepared by vacuum heating of a stoichiometric mixture of high-purity (99.999%) antimony and tellurium in a vacuum-sealed silica tube. The tube was heated gradually up to a temperature just above the melting points of both the metals and was kept at that temperature for 24 h. It was then cooled to just below the melting point of the Sb_2Te_3 alloy and was held at that temperature for 24 h and slowly cooled to room temperature. X-ray Debye-Scherrer photography revealed that the bulk Sb_2Te_3 alloy was crystalline and homogeneous. The substrates on which the films were prepared were glass plates held at room temperature, at a distance of about 30 cm vertically above the source of evaporation. Before the films were deposited, glass plates were cleaned with warm chromic acid, Teepol detergent solution, distilled water, and isopropyl alcohol, in that order. The vacuum evaporation was carried out in a vacuum better than 2×10^{-5} Torr. Films of different thicknesses were prepared in separate evaporations. In each case a given quantity of the bulk Sb_2Te_3 alloy was taken in the boat and was completely evaporated at a fast rate to avoid possible fractionization of the alloy and to maintain the average composition of the film, same as that of the bulk alloy Sb_2Te_3. Films of given thickness both for the electrical resistivity and the thermoelectric power measurements were prepared simultaneously using suitable masks. Lateral dimensions of the films were 6.5×0.5 cm^2 for thermoelectric power measurements and 3×1 cm^2 for electrical resistivity measurements. The thickness of the films was

 0021-8979/89/062332-10$02.40

measured with a quartz crystal monitor. The accuracy of the measurement was $\pm 2\%$.

It was found in previous studies[15] that the as-grown Sb_2Te_3 thin films formed on glass substrates at room temperature are amorphous and crystallize upon heating (at about 350 K), and as we wanted to study crystalline Sb_2Te_3 thin films, the as-grown thin films were annealed at 500 K for 1 h in vacuum and cooled before making either of the electrical measurements.

For the electrical resistivity measurements, Sn (tin) contact films were used, as it was found that the use of Ag and Cu films for the contacts led to a reaction with the Sb_2Te_3 film at the area of contact. The thick (~ 3000 Å) contact films were predeposited before the formation of the experimental film.

Electrical resistance of the film was measured using a Wheatstones bridge to an accuracy of 0.1%–1%, depending on the film resistance. The measurements were made at intervals of 2 K between 300 and 470 K. The error involved in the resistivity was about $\pm 5\%$, mainly because of the measurement errors in the dimensions of the film.

Thermoelectric measurements were made using the integral method in which one end of the film is kept at a constant low temperature and the other end is heated and the developed thermal emf is measured with respect to the temperature gradient. The thermoelectric power at a given temperature was determined as the derivative of the thermal emf plot (at that temperature).

The temperature and the thermal emf were measured using sensitive pontentiometers and null detectors (10^{-9} A/div). Copper-constantan thermocouples were used for the temperature measurements and the thermal emf of the Sb_2Te_3 thin film was measured with respect to copper. The error in the thermoelectric measurement was less than $\pm 1\%$. The experimental setup for the thermoelectric power measurement consisted of a massive copper block in thermal contact with the base plate of the vacuum system. One end of the experimental film was clamped to the copper block which acted as a thermal sink. The other end of the film could be clamped to a mini heater which could heat that end. The details of the experimental setup can be found in our earlier papers.[16–19] Both the electrical resistivity and thermoelectric power measurements were carried out in a vacuum better than 2×10^{-5} Torr.

The raw experimental data of resistance as a function of temperature and thermal emf developed as a function of temperature difference between the ends of the film were fitted using spline functions which are localized polynomials, so as not to force the experimental data to a predetermined relationship as a function of temperature. Thermoelectric power values at different temperatures were evaluated from the above least-squares-fitted curves of thermal emf versus temperature difference. From these experimental results, the resistivity and thermoelectric power of films of different thicknesses were evaluated at three different temperatures. These resistivity and thermoelectric power versus thickness data were fitted in the usual way as we expect from the theory that both of these depend on reciprocal thickness linearly.

III. RESULTS

Figures 1(a), 1(b), and 2 show, respectively, the Seebeck coefficient and resistivity variation with temperature during heating and cooling in the case of an as-grown Sb_2Te_3 thin film (thickness 800 Å). It is seen from the figures that in

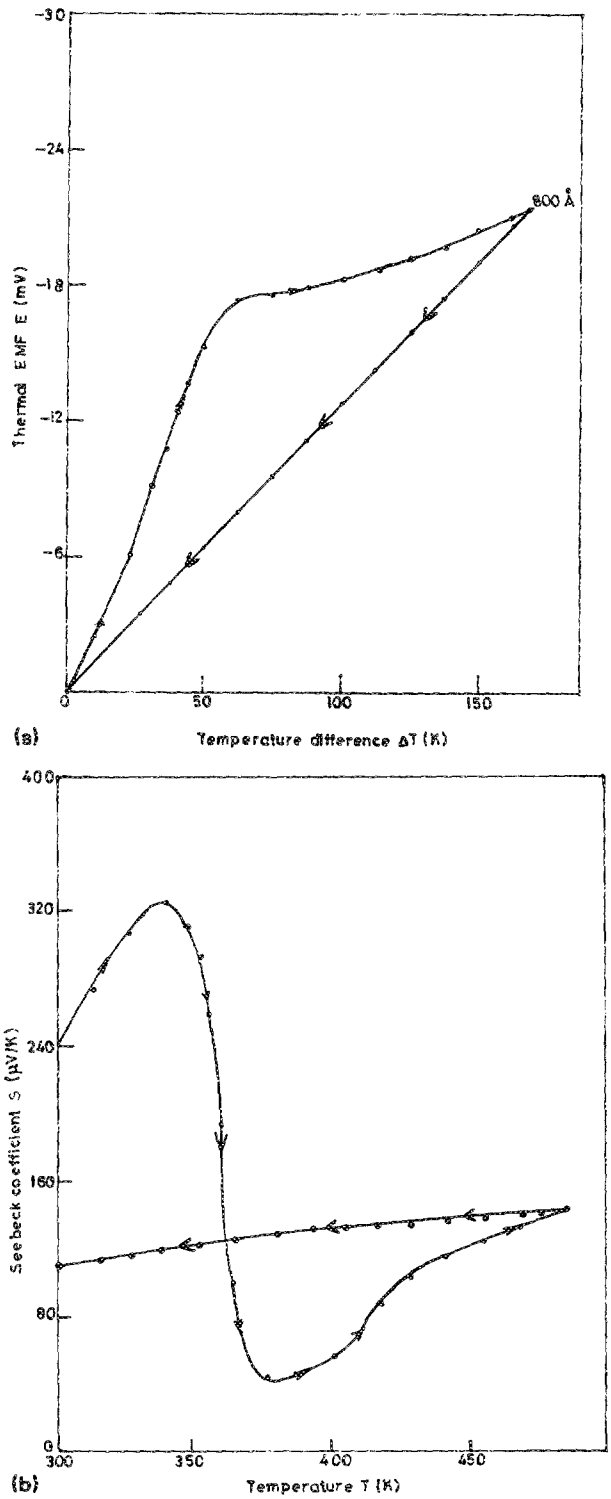

FIG. 1. (a) The variation of thermal emf as a function of temperature difference of unannealed (as-grown) thin film of thickness 800 Å during heating and cooling cycles. (b) The variation of the Seebeck coefficient as a function of temperature of unannealed (as-grown) thin film of thickness 800 Å during heating and cooling cycles.

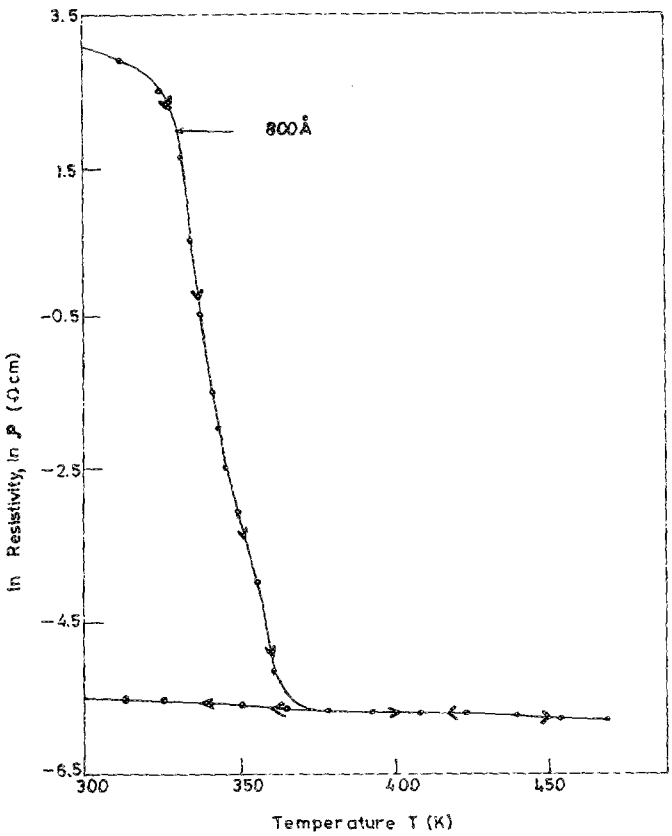

FIG. 2. The logarithmic variation of electrical resistivity as a function of temperature for unannealed (as-grown) film of thickness 800 Å.

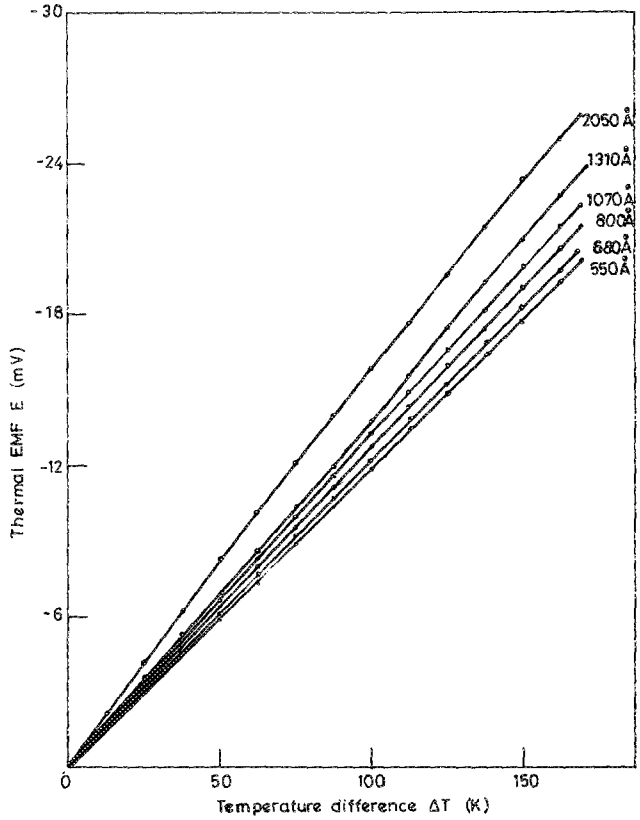

FIG. 3. The variation of thermal emf as a function of temperature difference for annealed (crystalline) thin films of different thicknesses.

both cases the temperature variations are different during heating and cooling. In the case of thermoelectric power, there is a sharp fall (by an order of magnitude) at around 350 K during heating. With a further rise in temperature, the thermoelectric power increases at a fast rate at first, and later, much more slowly. On cooling, it decreases nearly linearly with temperature without any sharp fall or increase at any point. Similarly, in the case of resistivity, there is a very sharp fall by several orders of magnitude at around the same temperature of 350 K during heating. With a further increase in temperature, the resistivity decreases very slowly. Upon cooling, resistivity increases steadily and very slowly with temperature, again without any sharp fall or increase at any point. Thus, it is evident that there is an irreversible change in the film on heating. This change is an amorphous-crystalline transition, as has been shown by us previously.[15] The changes occurring in the electrical resistivity and thermoelectric power of films of different thicknesses due to crystallization have already been discussed in our earlier paper[15] and hence need not be discussed here again. To avoid irreversible changes upon heating in electrical resistivity and thermoelectric power of the films and more particularly to study the behavior of these parameters (with respect to temperature and thickness) in crystalline Sb_2Te_3 thin films, the films were annealed at 500 K for 1 h after formation, and only then their electrical resistivity and thermoelectric power were measured.

The variation of the developed thermal emf as a function of temperature difference is shown in Fig. 3 for annealed (crystalline) films of different thicknesses. The calculated Seebeck coefficient (S) for annealed (crystalline) films of different thicknesses is plotted as a function of temperature in Fig. 4(a). To analyze the temperature dependence of thermoelectric power in detail, log S vs log T plots of the data were drawn as shown in Fig. 4(b). It is seen from Fig. 4(b) that there is a linear relationship between log S and log T with slope of about $\frac{1}{3}$, indicating that S varies as $T^{1/3}$. To study the variation of the Seebeck coefficient with respect to thickness (t), the Seebeck coefficient at 300 K was plotted against the reciprocal of thickness as shown in Fig. 5. The Seebeck coefficient of the films shows a linear dependence on inverse thickness. The best fit obtained by the least-squares error analysis is shown in the same figure.

In Fig. 6 the variation of the Seebeck coefficient as a function of the reciprocal of thickness at 300, 350, and 400 K is plotted. It is seen that S vs $1/t$ plots are linear at all three temperatures, within experimental error.

The variation of resistivity as a function of temperature is plotted in Fig. 7(a) for annealed (crystalline) films of different thicknesses. The data were analyzed further by plotting $\log(\rho T^{-3/2})$ vs $1/T$ plots. It was found that the plots were linear, as shown in Fig. 7(b). The slopes of the plots were between 0.26 and 0.30 leading to activation energies between 54 and 60 meV. Figure 8 gives the resistivity of these antimony telluride films at 300 K as a function of the reciprocal of thickness. The resistivity also shows a linear dependence on inverse thickness within experimental errors. Figure 9 shows the variation of resistivity as a function of inverse thickness for the films at three different temperatures

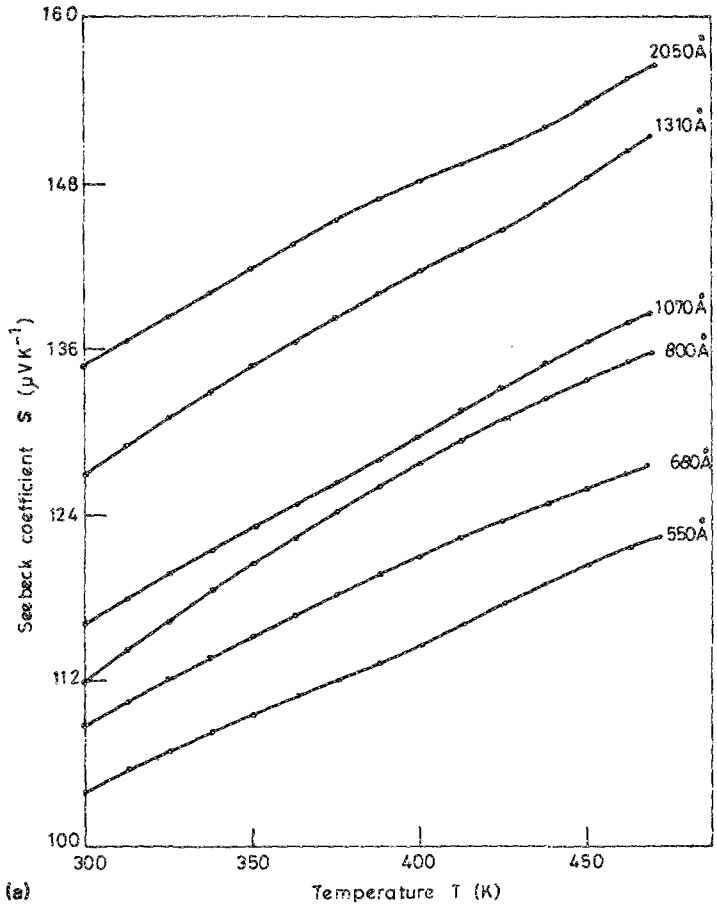

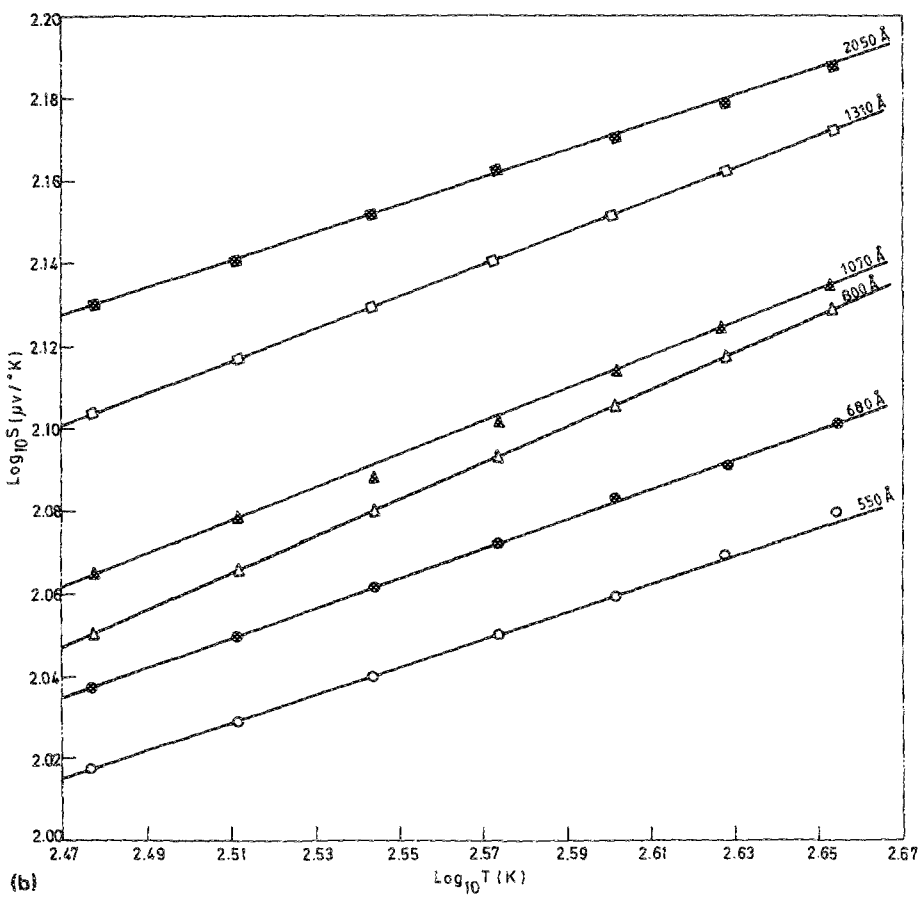

FIG. 4. (a) The variation of the Seebeck coefficient as a function of temperature for annealed (crystalline) thin films of different thicknesses. (b) log S vs log T plot of the thermoelectric power data for films of different thicknesses.

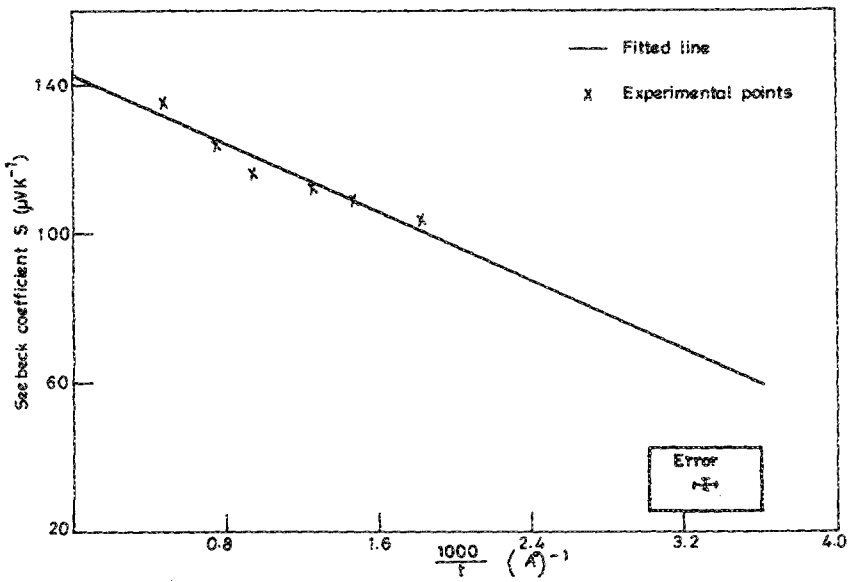

FIG. 5. The plot of Seebeck coefficient (at 300 K) of crystalline thin films as a function of reciprocal thickness.

(300, 350, and 400 K). It is seen that these plots are also linear at all three temperatures within experimental errors.

IV. DISCUSSION

A. Thermoelectric power

1. Temperature dependence

Studies on the Seebeck coefficient of antimony telluride confirm that antimony telluride is a p-type semiconductor irrespective of the kind of doping (Rajagopalan and Ghosh[12] and Champness, Chiang, and Parekh[20]). The films in our studies also had a positive Seebeck coefficient, confirming that the films are p type. In our films, the Seebeck coefficient is positive, temperature dependent, and thickness dependent.

In the case of a p-type semiconductor obeying Boltzmann statistics (i.e., nondegenerate semiconductor), the Seebeck coeffficient is given by Kireev[21]:

$$S=\frac{k}{e}\left(\frac{5}{2}+b-\frac{(E_F-E_V)}{kT}\right)$$
$$=\frac{k}{e}\left[\frac{5}{2}+b+\ln\left(\frac{N_V}{n}\right)\right],$$

where E_F is the Fermi energy, E_V is the energy of the top of the valence band, n is the carrier concentration, N_V is the density of states, and b is defined by

$$\tau=aE^b,$$

where τ, the relaxation time, is considered to be a function of energy, and a and b are constants. k is the Boltzmann constant, and e the charge on the carrier. Below 900 K, the material is extrinsic. At very low temperatures, the carriers will be activated from the impurity levels. At higher temperatures, i.e., in the impurity depletion region, $n=N_A$ is the acceptor concentration. Thus, the Seebeck coefficient expression reduces to

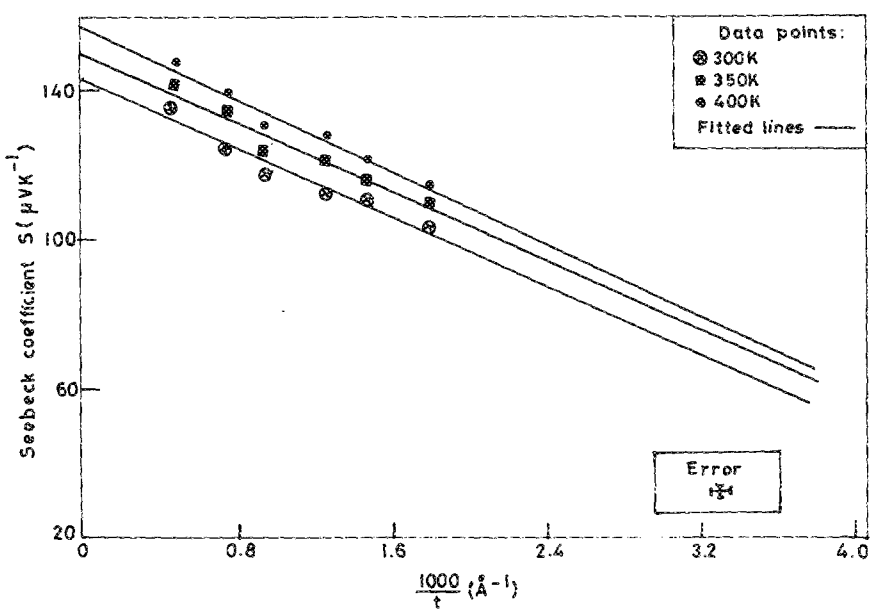

FIG. 6. The reciprocal thickness dependence of Seebeck coefficient at different temperatures (300, 350, and 400 K).

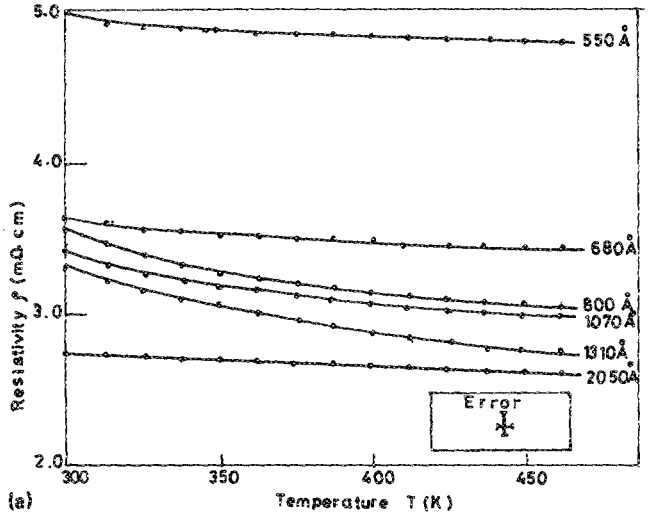

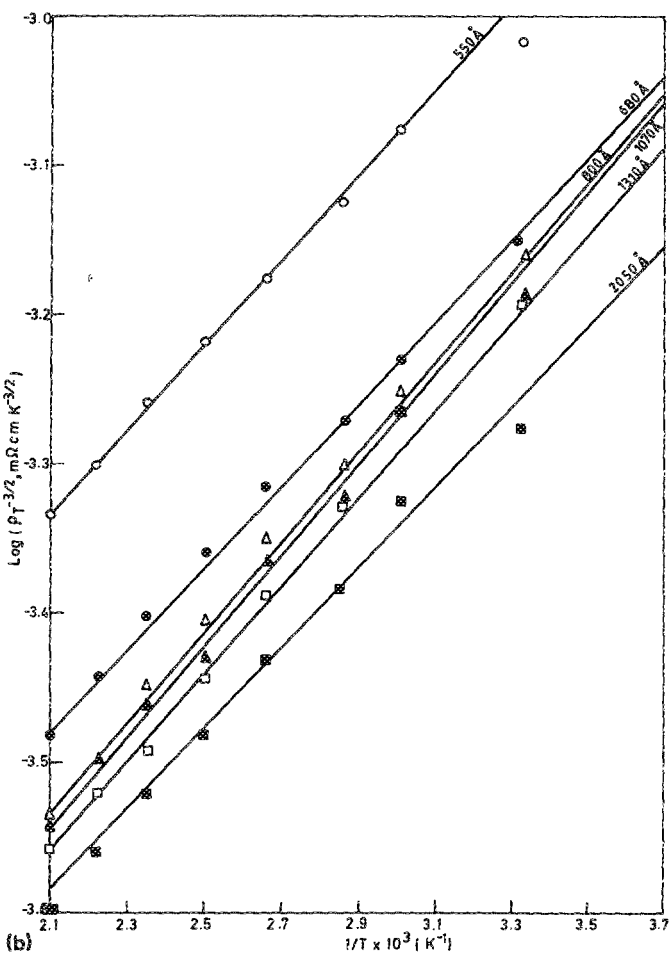

FIG. 7. (a) The variation of resistivity of annealed (crystalline) films as a function of temperature for different thicknesses. (b) $\log(\rho T^{-3/2})$ vs $1/T$ plot of the resistivity data for all the films of different thicknesses.

$$S=\frac{k}{e}\left[\left(\frac{5}{2}\right)+b+\ln\left(\frac{N_V}{N_A}\right)\right].$$

The effective density of states in the valence band is given by

$$N_V=2\left(\frac{2\pi m_i kT}{h^2}\right)^{3/2},$$

where m_i is the effective mass of the carriers, h the Planck's constant, and T the temperature in Kelvin. Since N_A is independent of temperature, the Seebeck coefficient increases with temperature. Our observations show that the Seebeck coefficient of annealed Sb_2Te_3 films increases with temperature for all thicknesses [Fig. 4(a)]. So, in the temperature range from 300 to 470 K, the film is in the impurity depletion region. This is further confirmed by the weak temperature dependence of electrical resistivity of the films in the above temperature range (Fig. 7). To analyze the nature of dependence of thermoelectric power on temperature, $\log S$ vs $\log T$ plots were drawn [Fig. 4(b)]. It is clear from Fig. 4(b) that $\log S$ vs $\log T$ plots are linear in the case of all the films, but slopes are equal to only about $\frac{1}{3}$. In the case of degenerate semiconductors (as in the case of metals), thermoelectric power S is given by

$$S=-(\pi^2k^2T/3eE_F)(1+U)$$

and hence is a linear function of temperature. Thus, our films show neither a nondegenerate semiconductor behavior nor a degenerate behavior, but a $\frac{1}{3}$ power temperature dependence.

2. Thickness dependence

Since the carrier concentration is almost independent of temperature, the transport properties can be discussed in terms of the free-electron theory. Models based on the free-electron theory to describe the behavior of the Seebeck coefficient as a function of thickness in thin films are many (Mayer,[22] Leonard and Lin,[23] Mikolajczak, Piasek, and Subotowcz,[24] Pichard, Tellier, and Tosser.[25]) Of these, the effective mean free path model developed by Pichard and coworkers[25] not only takes into account the grain boundary scattering in addition to external surface scattering, but also is simple and useful to carry out the analysis. In the effective mean-free-path model, the Seebeck coefficient as a function of thickness is given by[25] the asymptotic expression

$$S_f=S_g\left[1-\frac{3}{8}\frac{dg}{t}(1-p)\left(\frac{(\partial\ln l_g/\partial\ln E)E_F}{1+(\partial\ln l_g/\partial\ln E)E_F}\right)\right]$$

for $t>1$ where S_g, l_g, and $(\partial\ln l_g/\partial\ln E)E_F$ are the Seebeck coefficient, the mean free path, and the energy dependence of the mean free path U_g, respectively, in the infinite thick film. The infinite thick film is a hypothetical bulk having the same grain structure as that of the films. Even though the expression is valid for $t>l_g$, it is found to be valid, without much error, down to $t/l_g=0.1$, as numerically shown[26] (for $t/l_g=0.1$, error is only 7%). Hence, the above expression has been used for the size effect analysis of our thin films of thicknesses in the range 500–2000 Å, even though mean free path l_g turns out to be 2500 Å.

p is called the specularity parameter. It gives the fraction of the carriers incident on the surfaces that is specularly scattered by them, just as the light rays are reflected from a polished (mirror) surface. Specularly scattered carriers do not contribute to the size effect as they are not scattered randomly from the surfaces. Thus, maximum size effect is observed when $p=0$, i.e., when all the carriers are diffusely (randomly) scattered by the surfaces. In the present analysis p is assumed to be zero so that the maximum size effect is taken into account.

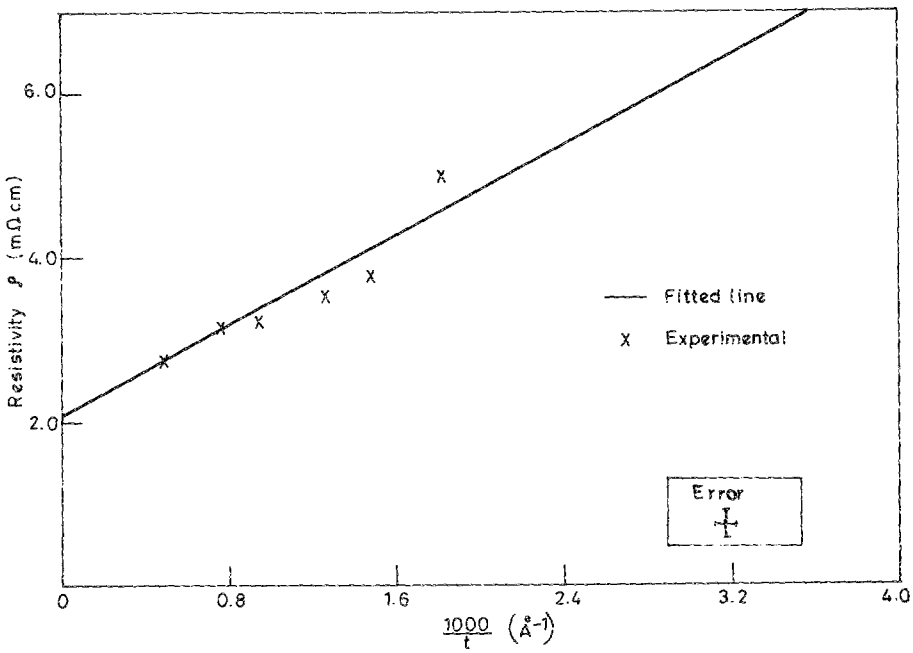

FIG. 8. The reciprocal thickness dependence of resistivity at 300 K of annealed (crystalline) thin films.

According to this model, the Seebeck coefficient depends on the reciprocal of thickness. From Fig. 5, which shows the experimental points and the linear fitting by least squares error analysis, and Fig. 6, which shows the linear fitting at different temperatures 300, 350, and 400 K, it can be said that the data are in reasonable agreement with the $1/t$ dependence. S_g is 143, 150, and 157 μV K^{-1} at 300, 350, and 400 K as determined by extrapolation of plots in Fig. 6. The maximum error involved in the estimation of the Seebeck coefficient of the infinite thick films is 5 μV K^{-1}. The slopes of the straight lines can be used to determine the mean free path or its energy dependence if either of them is known.

B. Electrical resistivity

1. Temperature dependence

The mean free path of the carriers in single crystals is available. However, the effective mean-free-path model presumes a hypothetical bulk where the material has the film grain structure. Since the mean free path of the carriers in a single crystal and the hypothetical bulk will differ noticeably because of the grain-boundary scattering, the use of the bulk mean free path in the calculations will lead to errors. To avoid this, the mean free path of the carriers in the infinite thick film can be determined from the studies on the thick-

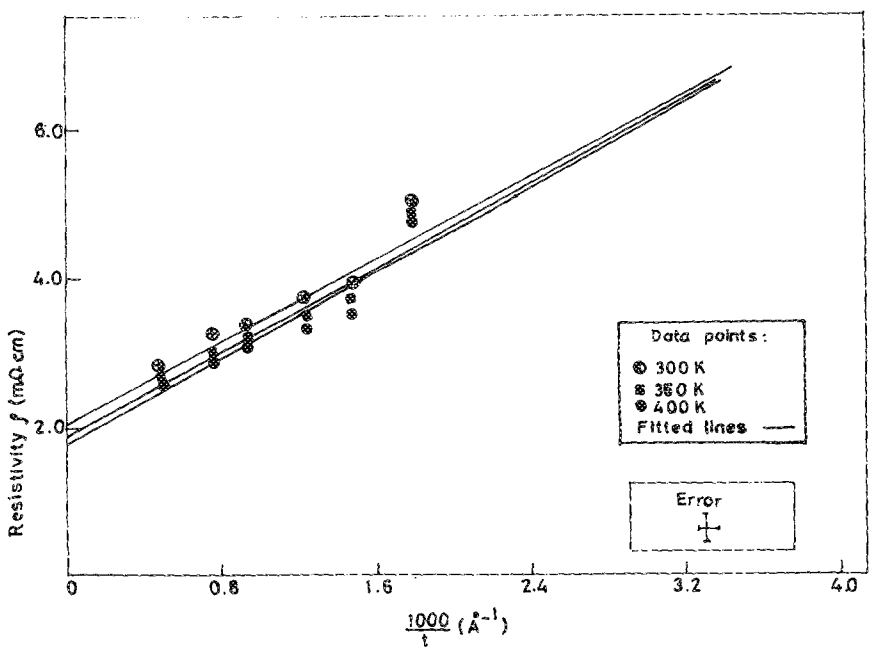

FIG. 9. The reciprocal thickness dependence of resistivity at different temperatures (300, 350, and 400 K).

TABLE I. Activation energy values of Sb_2Te_3 films of different thicknesses (from $\log \rho T^{-3/2}$ vs $1/T$ plots).

Film thickness (Å)	Activation energy (meV)
550	57
680	55
800	60
1070	60
1310	56
2050	54

ness dependence of the resistivity of the films prepared under identical conditions.

Therefore, studies were carried out to analyze the thickness dependence and the temperature dependence of the resistivity of the films of different thicknesses prepared under identical conditions.

From Fig. 7 it can be seen that the resistivity of the films is weakly temperature dependent. It slightly decreases with increasing temperature. Rajagopalan and Ghosh[12] observed a similar kind of temperature dependence of resistivity of thin films. But Brodovy and Lyashenko[7] found a slow increase in resistivity with increasing temperature. To analyze the temperature dependence of resistivity in detail, $\log(\rho T^{-3/2})$ vs $1/T$ plots were drawn [Fig. 7(b)]. It is seen in Fig. 7(b) that the plots are linear in all cases and the slopes yield activation energies varying between 54 and 60 meV, as shown in Table I. These values do not correspond to the band gap of the material (0.2 eV) and should therefore be attributed to impurity levels.

2. Thickness dependence

Sondheimer[27] analyzed the thickness dependence of resistivity of thin films taking into account the surface scattering of charge carriers. However, as is known, and mentioned earlier, thin films are generally polycrystalline and the average grain size is of the order of the film thickness. So, carriers are also significantly scattered by grain boundaries, in addition to the scattering by external surfaces. This requires that the discussion of the transport properties of the thin films should be carried out also taking into account the grain-boundary scattering. Mayadas and Shatzkes[28] modified the Fuchs–Sondheimer expression to discuss the film resistivity, taking into account the grain-boundary scattering. But the expression is complicated. Attempts have been made to simplify the analytical expression of the Mayadas–Shatzkes theory.

Tellier[29] has derived a simple analytical expression for the electrical resistivity as a function of thickness, by defining an effective mean free path of the carriers in the infinite thick film. According to this model, the film resistivity as a function of its thickness is given by

$$\rho_f = \rho_g \left[1 - \frac{3}{2} \frac{(1-p)}{K_g} \times \int_{-1}^{\infty} \left(\frac{1}{x^3} - \frac{1}{x^5} \right) \times \left(\frac{1 - \exp(-K_g x)}{1 - p \exp(-K_g x)} \right) dx \right]^{-1},$$

where ρ_g is the resistivity of the infinite thick film and l_g is the effective mean free path. K_g is the ratio of film thickness to mean free path l_g. In the asymptotic case, the expression simplifies to

$$\rho_f = \rho_g \{ 1 + \tfrac{3}{8} [(1-p) l_g / t] \},$$

where $K_g = t/l_g > 1$,

or

$$\sigma_f = \sigma_g \{ 1 - \tfrac{3}{8} [(1-p)/t] l_g \},$$

where

$$K_g = t/l_g > 1.$$

This expression, as shown numerically, holds for values down to $K_g \sim 0.1$. According to the equation, the plot of ρ_f vs $1/t$ will be a straight line. The intercept gives the bulk resistivity ρ_g. From the slope l_g, the effective mean free path can be determined. It is seen from Fig. 8, which gives the experimental points and the linear fitting by least squares error analysis according to this model, and Fig. 9, which gives the linear fitting of the experimental points at different temperatures, that the variation of resistivity with inverse thickness is in near agreement with that expected from the theory (nearly linear). The resistivity of the infinite thick film obtained from extrapolating these plots at 300, 350, and 400 K is, respectively, 2.1, 1.8, and 1.7 mΩ cm. The mean free path of the carriers in the hypothetical bulk at 300, 350, and 400 K is, respectively, 2700, 2500, and 2200 Å as obtained from these plots.

Rajagopalan and Ghosh[12] found that very thick films had the resistivity 1.8–2.0 mΩ cm. Benel[1] obtained single crystals of resistivity 40 mΩ cm. Ronnuld and co-workers[2] measured resistivities of single crystals of different doping to be in the range 2–5 mΩ cm. Thus, the resistivity value of the infinite thick films obtained from this study is in agreement with all of the values reported for very thick films and single crystals except with those obtained by Benel.[1] Here it should be pointed out that the resistivity of the material will vary if the stoichiometry is changed, and Benel's high value of 40 mΩ cm can be due to stoichiometry changes.

C. Estimation of parameters

Using the mean free path evaluated from the above analysis of resistivity-thickness dependence in the analysis of the size effect of the Seebeck coefficient to estimate $(\partial \ln l_g / \partial \ln E) E_F$, the exponent of the energy term in the energy-dependent mean free path can be evaluated. It is found to have values. 0.20, 0.25, and 0.20 at 300, 350, and 400 K, respectively.

Mayadas and Shatzkes[28] have shown that the product of ρ_g and l_g is equal to ρ_0 times l_0. From the free-electron theory,

$$\frac{1}{\rho_0 l_0} = \left(\frac{1}{3\pi^2} \right)^{1/3} \frac{e^2 n^{2/3}}{\hbar},$$

where n is the carrier concentration. Since ρ_g and l_g are known at 300, 350, and 400 K, carrier concentration can be estimated at these temperatures. The calculated concentrations are 1.8, 1.9, and 1.8×10^{17} carriers per cm^3.

In the effective mean free path model, the Sebeck coefficient of the infinite thick film is given by

TABLE II. Comparison of the evaluated parameters with the published results.

Serial No.	Parameter	Temperature (K)	Present work	Published results
1	Hole concentration (cm^{-3})	300	$(1.8 \pm 0.4) \times 10^{17}$	2.8×10^{17} (Ref. 5)
		350	$(1.9 \pm 0.4) \times 10^{17}$	2.0×10^{19} (Ref. 9)
		400	$(1.8 \pm 0.4) \times 10^{17}$	
2	Hole mean free path (Å)	300	2700 ± 200	
		350	2500 ± 200	
		400	2200 ± 200	
3	Fermi energy (eV)	300	0.060 ± 0.005	
		350	0.061 ± 0.005	
		400	0.057 ± 0.005	
4	Effective mass (m_e)	300	0.021 ± 0.004	0.073 (Ref. 5)
		350	0.020 ± 0.004	
		400	0.021 ± 0.004	
5	S_g (μV/K)	300	143 ± 3	
		350	150 ± 3	
		400	157 ± 3	
6	ρ_g (mΩ cm)	300	2.1 ± 0.2	
		350	1.8 ± 0.02	1.8–2 (Ref. 12), 2–5 (Ref. 2), 40 (Ref. 1)
		400	1.7 ± 0.02	(bulk) (bulk)
7	$\left(\frac{\delta \ln l_g}{\delta \ln E}\right) E_F$	300	0.20 ± 0.02	
		350	0.25 ± 0.02	
		400	0.20 ± 0.02	

$$S_g = \frac{-\pi^2 k^2 T}{3eE_F}\left[1 + \left(\frac{\delta \ln l_g}{\partial \ln E}\right) E_F\right].$$

As S_g and $(\partial \ln l_g / \partial \ln E) E_F$ are known, E_F can be calculated. It is found that at the temperatures 300, 350, and 400 K, E_F is constant and is equal to 0.06 eV. Using the expression

$$E_F = (\hbar^2/2m^*)(3\pi^2 n)^{2/3},$$

the effective mass of the carriers can be calculated using the evaluated values of Fermi energy and the carrier concentration at different temperatures. It turns out that the effective mass is independent of temperature and is equal to 0.02 m_0, where m_0 is the rest mass of the electrons.

The estimated values are tabulated in Table II and compared with the published data. Also included in the table are the estimated errors involved in the calculations of the parameters due to experimental errors. It is seen that the carrier concentration and resistivity values are in reasonable agreement, while for the effective mass, only an order of magnitude agreement is found. The low value of the effective mass obtained (0.02 cm) may be because of the use of the free electron theory expression for the thermoelectric power, viz.,

$$S = \left(-\frac{\pi^2 k^2 T}{3eE_F}\right)(1 + U).$$

As we have seen earlier, S is not a linear function of temperature as this expression suggests, but is given by $S = \text{const}\ T^{1/3}$. Thus, the use of free-electron theory expression leads to only an order of magnitude value of the effective mass. A comparison of the values obtained for the different parameters with the values obtained for Bi_2Te_3 (Ref. 30) show the following: (1) The carrier concentration (in the present case holes instead of electrons) is nearly the same (at 400 K) as that of Bi_2Te_3, but it remains nearly constant with temperature, unlike in the case of Bi_2Te_3. (2) The mean-free-path value (at 300 K) is about half that in Bi_2Te_3 (2700 vs 5500 Å) but slowly varies with temperature, unlike the case of Bi_2Te_3. (3) The Fermi energy is nearly the same as for Bi_2Te_3. (4) The effective mass (at 400 K) is nearly the same as that of electrons in Bi_2Te_3 but is not a function of temperature increasing with it, but is nearly constant. (5) The thermoelectric power is of the same magnitude (+ 143 vs $-130\,\mu$V/K) but increases more steeply with temperature. (6) The resistivity values are about double that of Bi_2Te_3 thin films.

V. CONCLUSIONS

Antimony telluride thin films of different thicknesses between 500 and 2000 Å have been studied. Only the annealed crystalline films were used to study the Seebeck coefficient and the electrical resistivity behavior in them. The data were analyzed on the basis of the effective mean-free-path model. It has been found that both the Seebeck coefficient and the electrical resistivity are thickness dependent, varying nearly linearly with inverse thickness. The parameters such as carrier concentration, mean free path, effective mass, and Fermi energy have also been determined. Some of these calculated values have been compared with the values available in the literature.

[1] H. Benel, C. R. Acad. Sci. **247**, 584 (1958).
[2] B. Ronnlud, O. Beckman, and H. Levy, J. Phys. Chem. Solids **26**, 1282 (1965).
[3] R. Jaschke, Ann. Phys. **15**, 106 (1964).
[4] N. K. H. Abrikosov, L. D. Invanov, and T. I. Festisova, Inorganic Mater. **12**, 689 (1976).
[5] B. Roy, B. R. Chakraborty, R. Bhattacharya, and A. K. Dutta, Solid State Commun. **25**, 617 (1978).
[6] J. E. Mahan and R. H. Bube, J. Non-Cryst. Solids **24**, 29 (1977).
[7] V. A. Brodovyi and V. I. Lyaskenko, Ukr. Fiz. Zh. **6**, 664 (961).

[8]V. S. Tyushev and O. V. Shelud'ko, Izv. Vuz. Fiz. **3**, 46 (1967).
[9]M. M. Abou Sekkina, Ind. J. Phys. **53A**, 444 (1979).
[10]A. A. Averkin, B. M. Gol'tsman, Zh. Zh. Zhaparov, and V. A. Kutasov, Sov. Phys. Solid State **12**, 2726 (1972).
[11]L. G. Khostantsev, A. I. Orloo, N. Kh. Abrokosov, and L. D. Ivanova, Phys. Status Solidi (A) **58**, 37 (1980).
[12]N. S. Rajagopaian and S. K. Ghosh, Physics **29**, 234 (1963).
[13]L. H. Gadgil and A. Goswami, J. Vac. Sci. Technol. **6**, 591 (1969).
[14]V. A. Kremnev, P. A. Leont'ev, and A. I. Platov, Kristolliogr. **16**, 411 (1976).
[15]V. Damodara Das, N. Soundararajan, and M. Pattabi, J. Mater. Sci. **22**, 3522 (1987).
[16]V. Damodara Das and J. Chandra Mohanty, J. Appl. Phys. **54**, 977 (1983).
[17]V. Damodara Das, N. Jaya Prakash, and N. Soundararajan, J. Mater. Sci. **16**, 3331 (1981).
[18]V. Damodara Das and K. Seetharama Bhat, J. Appl. Phys. **55**, 1023 (1984).
[19]V. Damodara Das and D. Karunakaran, Phys. Rev. B **30**, 2036 (1984).
[20]C. H. Champness, P. T. Chiang, and P. Parekh. Can. J. Phys. (Paris) **43**, 653 (1965).
[21]P. S. Kireev, *Semiconductor Physics* (Mir, Moscow, 1978), p. 258.
[22]H. Mayer, in *Structure and Properties of Thin Films*, edited by C. A. Neugebauer and J. B. Newkirk (Wiley, New York, 1959), p. 225.
[23]W. F. Leonard and S. F. Lin, J. Appl. Phys. **41**, 1868 (1970).
[24]P. Mikolajczak, W. Piasek, and M. Subotowcz, Phys. Status Solidi A **25**, 619 (1974).
[25]C. R. Pichard, C. R. Tellier, and A. J. Tosser, J. Phys. F **10**, 2009 (1980).
[26]K. L. Chopra, *Thin Film Phenomena* (McGraw-Hill, New York, 1969), pp. 350–351.
[27]E. H. Sondeimer, Adv. Phys. **1**, 1 (1952).
[28]A. F. Mayadas and M. Shatzkes, Phys. Rev. B **1**, 1382 (1970).
[29]C. R. Tellier, Thin Solid Films **51**, 311 (1978).
[30]V. Damodara Das and N. Soundararajan, Phys. Rev. B **37**, 4552 (1988).